## Title

Electrochemical properties of poly(ethylene oxide) electrolytes above the entanglement threshold



## Authors

Gao, Kevin W
Balsara, Nitash P

## Publication Date

2021-06-01

## DOI

10.1016/j.ssi.2021.115609

Peer reviewed

# Electrochemical properties of poly(ethylene oxide) electrolytes above the entanglement threshold

Kevin W. Gao[a,b,c] and Nitash P. Balsara[*,a,b,c]

[a] *Department of Chemical and Biomolecular Engineering, University of California, Berkeley, Berkeley, California 94720, USA*

[b] *Materials Sciences Division, Lawrence Berkeley National Laboratory, Berkeley, California 94720, USA*

[c] *Joint Center for Energy Storage Research (JCESR), Argonne National Laboratory, Lemont, Illinois 60439, USA*

[*] Correspondence to: nbalsara@berkeley.edu

## Highlights

- Complete electrochemical characterization with 95% confidence intervals
- Polymer electrolytes were studied above the entanglement threshold
- Ion transport is independent of molecular weight above the entanglement threshold
- Sampling electrolytes with different molecular weights enables greater precision
- Negative cation transference numbers shown for a range of salt concentrations

## Abstract

Ion transport in electrolytes depends on three transport coefficients, conductivity ($\kappa$), salt diffusion coefficient ($D$), and the cation transference number with respect to the solvent velocity ($t_{+¿^0¿}$), and the thermodynamic factor ($T_f$). Current methods for determining these parameters involve four separate experiments, and the coupled nature of the equations used to determine them generally results in large experimental uncertainty. We present data obtained from 64 independent polymer electrolytes comprising poly(ethylene oxide) (PEO) and lithium bis(trifluoromethanesulfonyl)imide (LiTFSI) salt. The molecular weights of PEO ranged from 5 to 275 kg mol$^{-1}$; these samples are all above the entanglement threshold. We minimize the experimental uncertainty in transport and thermodynamic measurements by exploiting the fact that ion transport in entangled polymer electrolytes should be independent of molecular weight. The dependence of $\kappa$, $D$, $t_{+¿^0¿}$, and $T_f$ as a function of salt concentration in the range $0.035 \leq r \leq 0.30$ are presented with a 95% confidence interval, where $r$ is the molar ratio of lithium ions to ethylene oxide monomer units. While $\kappa$, $D$, and $T_f$ are all positive as required by thermodynamic constraints, there is no constraint on the sign of $t_{+¿^0¿}$. We find that $t_{+¿^0¿}$ is negative in the salt concentration range of $0.093 \leq r \leq 0.189$.

## Keywords

Polymer electrolyte

Ion transport

Entanglement molecular weight

## 1. Introduction

A complete description of ion transport in electrolytic mixtures was first provided by Onsager, who recognized the importance of three independent transport parameters that we refer today as Onsager coefficients.[1] These coefficients quantify frictional interactions between the cation and solvent, anion and solvent, and anion and cation. Measuring these transport coefficients is, however, nontrivial and beyond the scope of Onsager's original work. Newman developed concentrated solution theory based on the Onsager approach and recast ion transport in terms of three different but related transport coefficients: ionic conductivity ($\kappa$), salt diffusion coefficient ($D$), and cation transference number with respect to the solvent velocity ($t_{+¿^0¿}$).[2] In addition, it is necessary to measure the thermodynamic factor ($T_f$) which quantifies the dependence of the mean molal activity coefficient of the electrolyte, $\gamma_\pm$, on salt concentration ($\frac{d \ln \gamma_\pm}{d \ln (m)}$), where $m$ is the molality. Newman's approach is powerful because each of the four parameters $\kappa$, $D$, $t_{+¿^0¿}$, and $T_f$ can be determined from a set of well-defined experiments.[3]

While we focus on Newman's approach for characterizing ion transport, it is one of many frameworks proposed in the literature.[4–13] Some of these approaches employ different definitions for diffusion coefficients and transference numbers. For completeness, we clarify the definitions of these two parameters that are used in this paper, as specified in ref. 2. (1) The salt diffusion coefficient, $D$, is the proportionality factor that relates the flux density of salt to the concentration gradient. (2) The cation transference number with respect to the solvent velocity, $t_{+¿^0¿}$, is the

fraction of ionic current carried by the cation relative to the solvent velocity in an electrolyte of uniform composition, *i.e.,* the cation velocity needed to calculate ionic current is determined using the solvent velocity as the reference. Even though $t_{+¿^0¿}$ is defined for a solution of uniform composition, it is a property that can be used to quantify transport in electrolytes which are not of uniform composition, but it no longer represents the fraction of the current carried by the cation.[2] There is no ambiguity in the definitions of either conductivity, $\kappa$, or the mean molal activity coefficient of the electrolyte, $\gamma_{\pm}$.

The Onsager-Newman approach applies to any mixture of charged species in a neutral solvent such as a low molecular weight liquid or a high molecular weight polymer. An example of an electrolyte of interest for rechargeable lithium batteries is a mixture of a lithium salt such as lithium hexafluorophosphate ($LiPF_6$) dissolved in a suitable organic solvent such as propylene carbonate (PC); commercial batteries employ a mixture of carbonate solvents.[14–17]

The passage of current through a battery results in the formation of concentration gradients within the electrolytic phase. The rate at which batteries can be charged and discharged is limited by the magnitude of these gradients. The limiting current is typically defined as the current at which the ion concentration at the cathode (we assume that the working ion is a cation) approaches zero. Operating a battery at currents that exceed this value can result in rapid degradation and, in some cases, catastrophic failure. Similar problems arise if the salt concentration at the anode exceeds the solubility limit.[18,19] Concentration gradients in a battery electrolyte can only be predicted if $\kappa$, $D$, $t_{+¿^0¿}$, and $T_f$ are known functions of salt concentration.[19–21]

The Newman approach for measuring transport coefficients involves four separate experiments.[3] Conductivity, $\kappa$, is obtained from a relatively straightforward experiment via ac

impedance measurements using blocking electrodes. For the case of 1 M $LiPF_6$/PC electrolytes at 25 °C, $\kappa$ is consistently reported[22–27] to lie between 5.9 x $10^{-3}$ to 6.4 x $10^{-3}$ S $cm^{-1}$. Measuring the other transport parameters for lithium battery electrolytes requires the construction of lithium/electrolyte/lithium symmetric cells. The data obtained from these cells is inherently more complex due to the extreme reactivity of lithium, formation of the solid electrolyte interphase between lithium metal and all known electrolytes, and the instability of the lithium/electrolyte interface during electrochemical plating.[28–30] Of the remaining parameters, the salt diffusion coefficient, $D$, is most straightforward to measure because it is obtained directly from restricted diffusion experiments. In spite of this, the reported[24,26,27] value of the salt diffusion coefficient, $D$, in 1 M $LiPF_6$/PC electrolytes at 25 °C varies significantly, from 1.8 x $10^{-6}$ to 4.0 x $10^{-6}$ $cm^2$ $s^{-1}$. Determining $t_{+}^{0}$ and $T_f$ is further complicated because they are determined by combining results from two separate experiments, one involving a symmetric cell and the other involving a concentration cell where two electrolytes at different salt concentrations are coupled together between lithium electrodes.[3] The symmetric cell is used to obtain the steady-state current fraction, $\rho_+$, the ratio of current obtained under steady dc polarization to that obtained in the absence of concentration polarization.[31] The concentration cell is used to measure the dependence of the open circuit potential, $U$, on salt concentration ($\frac{dU}{d\ln(m)}$). If we combine the values of $D$ given above for 1 M $LiPF_6$/PC with typical values[22–27,32,33] for $\kappa$ (6.1 x $10^{-3}$ S $cm^{-1}$), $\rho_+$ (0.33), and $\frac{dU}{d\ln(m)}$ (-90 mV $\ln(m)^{-1}$), the estimated values of $t_{+}^{0}$ are 0.36 and -0.43. In other words, the uncertainty in salt diffusion coefficient, which by itself seems reasonable, is so large that even the sign of $t_{+}^{0}$ cannot be determined.

While there are many reports of $\kappa$, $D$, $t_{+}^{0}$, and $T_f$ in the literature, a detailed analysis of the uncertainty in the reported values is seldom mentioned. In this paper, we report the values of these parameters obtained in a standard polymer electrolyte, a mixture of poly(ethylene oxide) (PEO) and lithium bis(trifluoromethanesulfonyl)imide (LiTFSI) salt. We present data obtained at 90 °C from polymers with molecular weights ranging from 5 to 275 kg mol$^{-1}$. We define a salt concentration $r$ as the molar ratio of lithium ions to ethylene oxide repeat units. Our study covers salt concentrations in the range $0.005 \leq r \leq 0.3$. In these electrolytes, the PEO chains are entangled; the critical molecular weight for entanglement in these polymer chains is 2 kg mol$^{-1}$.[34,35] The importance of chain entanglement in polymer electrolytes was first recognized by Shi and Vincent.[36] A previous study[37] showed that $\kappa$ of PEO/LiTFSI at a fixed salt concentration was independent of polymer molecular weight above the entanglement threshold, an experimental observation corroborated by molecular dynamics simulations[38]. In this paper, we show that this is more or less true at all salt concentrations. In addition, $D$, $\rho_+$, $\frac{dU}{d\ln(m)}$, $t_{+}^{0}$, and $T_f$ are also more or less independent of molecular weight above the entanglement threshold at all salt concentrations. An important but rarely mentioned advantage of polymer electrolytes, then, is the capability to measure electrolyte properties using experiments that cover a wide range of molecular weights above the entanglement threshold, and average the data obtained from the different electrolytes, thereby reducing experimental uncertainty. In contrast, in the case of liquid electrolytes such as 1 M $LiPF_6$/PC, properties can only be measured at a single solvent molecular weight.

## 2. Methods

## 2.1 Electrochemical Characterization

$\kappa$ is determined by ac impedance spectroscopy of electrolytes with blocking electrodes. Measuring $D$ and $\rho_+$ require lithium/electrolyte/lithium symmetric cells: $D$ is measured by restricted diffusion[39] and $\rho_+$ via the Bruce-Vincent[40,41] method. $U$ is measured by monitoring the open circuit potential of a concentration cell in which an electrolyte of salt concentration $m$ is contacted together with a reference electrolyte of $r$ = 0.06 or $m$ = 1.38 kg mol$^{-1}$. $\frac{dU}{d\ln(m)}$ can be obtained from the slope of a plot of $U$ with respect to the natural logarithm of $m$.

The thermodynamic factor, $T_f$, is given by the following equation:

$$T_f = \frac{\kappa}{2RTDc¿¿¿}$$

where $R$ is the gas constant, $T$ is the temperature, and $c$ is the molarity. The cation transference number is given by the following equation:

$$t_{+¿^0} = 1 - t_{-¿^0} = 1 - \frac{FDc}{\kappa\left(\frac{dU}{d\ln m}\right)}¿¿¿$$

where $t_{-¿^0¿}$ is the anion transference number and $F$ is the Faraday constant.

Data was taken from previously published results which also include more detailed experimental procedures for measuring each transport parameter (see Table 1).[21,42–46] Data used in this report, and their units of measurement, is provided in the Supplementary Information (SI).

**Table 1**. PEO molecular weights in PEO/LiTFSI electrolytes

| Molecular Weight (kg mol$^{-1}$) | Reference(s) |
|---|---|
| 5 | Pesko et al.<br>Chintapalli et al. |
| 10 | Hoffman et al. |

| | |
|---|---|
| 35 | Gribble et al. |
| 100 | Zheng et al. |
| 275 | Pesko et al. |

### 2.2 Error propagation

The electrochemical data shown at each specific molecular weight and salt concentration is the average of at least three measurements in as many different samples. The error bars are the standard deviation of the measured values among the samples. We use standard error propagation for $t_{+}^{0}$, assuming independent variables and neglecting correlations.[47] The error for $t_{+}^{0}$, then, is given by a simplified expression:

$$\delta t_{+}^{0} = \quad$$

where ¿ is the magnitude of the anion transference number and the standard deviations for each electrochemical measurement are given by $\delta\kappa$, $\delta D$, $\delta\rho_{+}$, and $\delta\frac{dU}{d\ln(m)}$. Note that the first term of the right side of Equation 3 is the magnitude of the anion transference number, and we also include error from the concentration cell data, facts that were missed in ref [42]. $\delta\kappa$, $\delta D$, and $\delta\rho_{+}$ are experimental standard deviations while $\delta\frac{dU}{d\ln(m)}$ is approximated from the fit of the experimental concentration cell data by using each fit coefficient's standard deviation and applying standard error propagation.[47]

## 3. Results and Discussion

Figure 1 plots the electrochemical properties $\kappa$, $D$, $\rho_{+}$, and $U$ of PEO/LiTFSI electrolytes as a function of PEO molecular weight. Five representative salt concentrations are shown ($r$ =

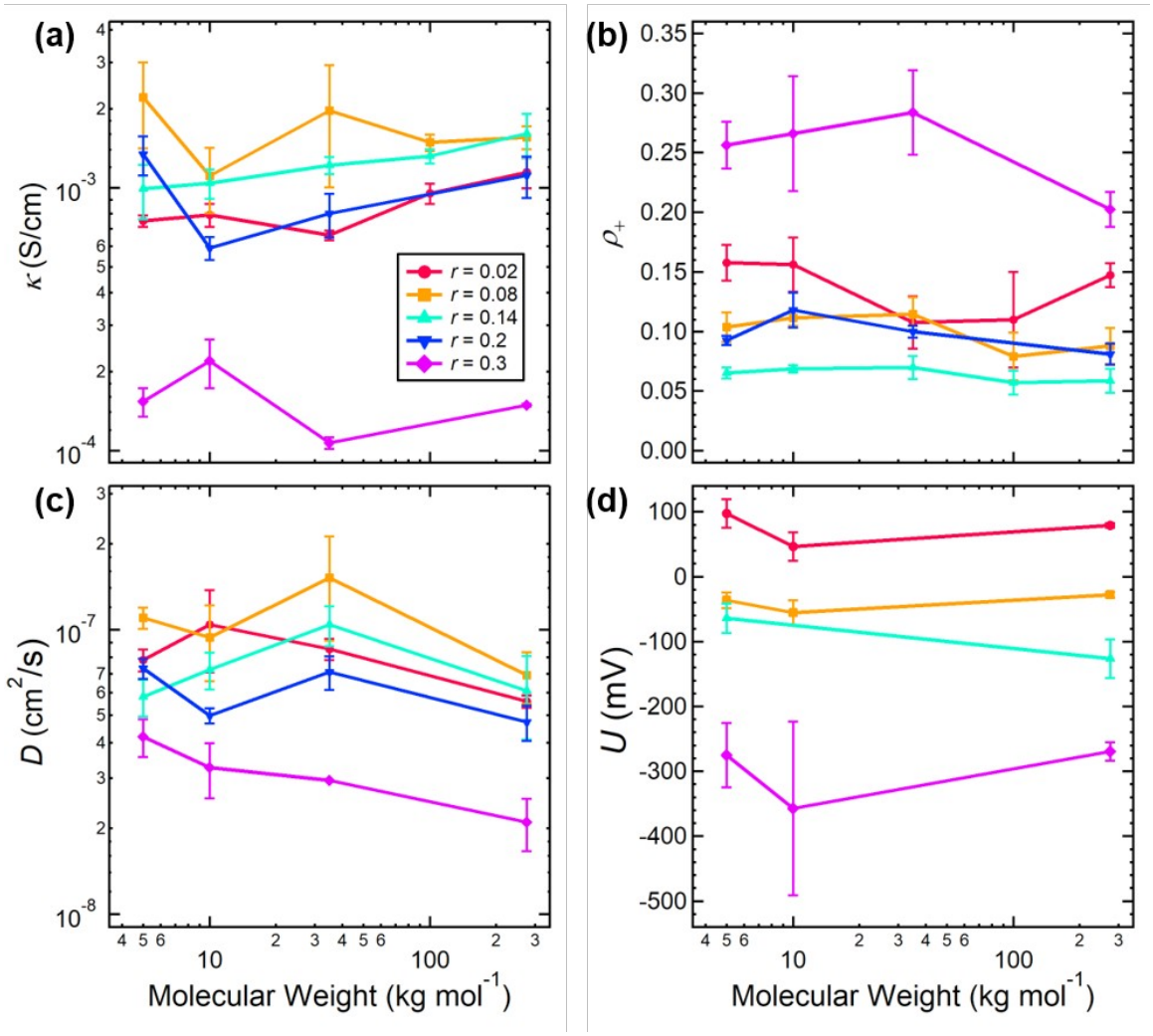


0.02, 0.08, 0.14, 0.2, and 0.3). As expected, none of the properties shown in Figure 1 exhibit discernible and systematic dependence on molecular weight.

**Figure 1.** Molecular weight dependence of PEO/LiTFSI electrolytes at representative salt concentrations at 90 °C (circles/$r$ = 0.02; squares/$r$ = 0.08; triangles/$r$ = 0.14; inverted triangles/$r$ = 0.2; diamonds/$r$ = 0.3) for (a) ionic conductivity, $\kappa$, (b) current fraction, $\rho_+$, (c) salt diffusion coefficient, $D$, and (d) open circuit potential from concentration cells, $U$. Each data point in (a) – (d) represents the average of at least 3 independent samples and the error bars correspond to the standard deviation.

Figure 2a shows $\kappa$ of PEO/LiTFSI electrolytes as a function of salt concentration. The curve was obtained by fitting an expression for conductivity proposed by Mongcopa et al.[48] through the entire data set:

$$\kappa = 0.058\, r \exp\left(\frac{-r}{0.075}\right)\left[\frac{S}{cm}\right]. \quad (4)$$

At low salt concentrations, $\kappa$ increases with increasing $r$ due to the increase in charge carrier concentration. Equation 4 has an analytical maximum at $r$ = 0.075, consistent with several reports on PEO electrolytes.[49–53] The maximum is obtained because segmental motion, which plays an important role in ion transport, becomes slower with added salt.[54,55]

Figure 2b shows the dependence of $\rho_+$ on $r$. The curve was obtained by fitting the entire data set to a 2nd order polynomial:

$$\rho_{+} = 0.178 - 1.79\, r + 7.25\, r^2. \quad (5)$$

Equation 5 has an analytical minimum at $r$ = 0.123, consistent with several reports in the literature.[52,56] Computer simulations suggest that the non-monotonic dependence of $\rho_+$ on $r$ is due to the formation of transient, negatively charged ion clusters.[57,58] Equation 5 is remarkably similar to the fit reported by Galluzzo et al. for a series of mixtures of polystyrene-*b*-poly(ethylene oxide) copolymers and LiTFSI.[59]

Figure 2c shows the dependence of $D$ as a function of $r$. The curve was obtained by fitting the entire data set to a 2nd order polynomial:

$$D = \left(7.46 * 10^{-8}\right) + \left(2.75 * 10^{-7}\right) r - \left(1.41 * 10^{-6}\right) r^2 \left[\frac{cm^2}{s}\right]. \quad (6)$$

$D$ is a weak function of salt concentration in the range $0 < r < 0.20$. Equation 6 gives a weak analytical maximum at $r$ = 0.098, which is consistently seen at all molecular weights (see Figure 2c).

Finally, we plot $U$ as a function of $\ln(m)$ in Figure 2d. The abscissa was chosen because the quantity of interest is $\frac{dU}{d\ln(m)}$. The curve was obtained by fitting all data points to a power law equation:

$$U = 100 - 74.9\, m^{0.84}\,[mV]. \quad (7)$$

Equation 7 has no analytical maximum or minimum within the salt concentrations measured, but there is an analytical zero found at $m = 1.41$ which corresponds to $r = 0.062$, closely matching the reference electrolyte concentration of $r = 0.06$, as expected.

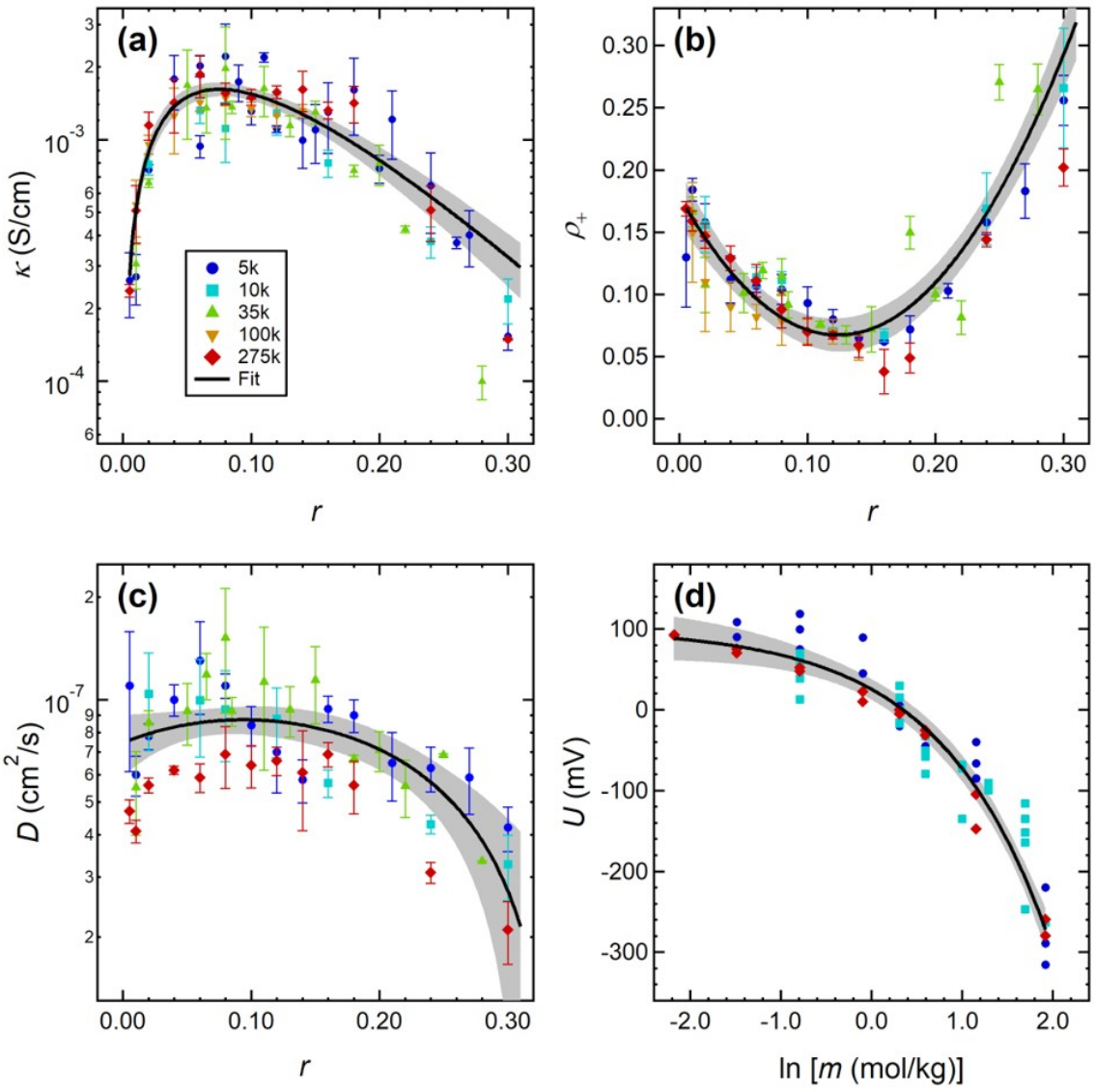

**Figure 2.** Electrochemical measurements of PEO/LiTFSI electrolytes at 90 °C for different salt concentrations and molecular weights (circles/5 kg $mol^{-1}$; squares/10 kg $mol^{-1}$; upward pointing triangles/ 35 kg $mol^{-1}$; downward pointing triangles/100 kg $mol^{-1}$; diamonds/275 kg $mol^{-1}$). The black line represents a fit through the entire data set. 95% confidence intervals for each fit are given by the gray shading. (a) Ionic conductivity, $\kappa$, from ac impedance spectroscopy of blocking electrode cells. (b) Current fraction, $\rho_+$, from applying the Bruce-Vincent method to lithium symmetric cells. (c) Salt diffusion coefficient, $D$, from using restricted diffusion method with lithium symmetric cells. (d) Measured open circuit potential, $U$, from concentration cells. Each data point in (a) – (c) represents the average of at least independent 3 samples and the error bars correspond to the standard deviation. Each data point in (d) is an independent sample.

The uncertainty of the fits in Figure 2 are represented by a 95% confidence interval and shown as gray shading surrounding the fitted curves. They represent the uncertainty of the fitted Equations 4-7 based on the entire set of 64 samples. Details of our approach are given in the SI.

The curves shown in Figure 2 are parsimonious fits of the experimental data. In the case of conductivity, which has been studied extensively, the fit parameters in Equation 4 reflect understanding of ion transport at the molecular level. The molecular underpinnings of the fit parameters in Equations 5-7 remain to be established. There is no molecular basis for the assumed functional forms of these equations.

We can use the data and fits in Figure 2 to calculate the cation transference number with respect to solvent velocity, $t_{+¿^0¿}$ from Equation 2 and the thermodynamic factor, $T_f$, from Equation 1. Figure 3a shows $t_{+¿^0¿}$ as a function of $r$. The curve was obtained by substituting Equations 4-7 into Equation 2. The data were obtained by inserting the measured values $\kappa$, $D$, $\rho_+$, and $\frac{dU}{d\ln(m)}$ directly into Equation 2. The large uncertainty in the data is due to the propagation of error in individual experiments, quantified by Equation 3. The uncertainty of the curve, however, is much less as it is based on data from 64 electrolytes created from polymers with

widely differing molecular weights. Our analysis shows that $t_{+}^{0}$ is a non-monotonic function of salt concentration. At values $0.093 \leq r \leq 0.189$, $t_{+}^{0}$ is negative. A negative $t_{+}^{0}$ means that when an electric field is applied to a PEO/LiTFSI mixture in this salt concentration range, the initial velocity of the cation and anion, measured using the solvent velocity as a reference, points toward the positive electrode. The implication is that in this range of salt concentrations, ion transport is dominated by negatively charged clusters.[57,58,60–64] The phenomenon of triple ions or higher associates that may carry a net charge that is opposite to the “central" ion is well-known in electrochemistry.[65–68] For $r > 0.189$, we see an increase in $t_{+}^{0}$ to positive values, which could be attributed to the breakup of negatively charged clusters.

Figure 3b shows $T_f$ as a function of $r$. The curve was obtained by substituting Equations 4-7 into Equation 1. The data were obtained by inserting the measured values $\kappa$, $D$, $\rho_+$, and $\frac{dU}{d\ln(m)}$ directly into Equation 1. The dependence of $T_f$ on $r$ falls into two regimes. In the regime $r < 0.17$, $T_f$ is small and is a weak function of $r$. This implies that the dependence of the salt activity coefficient on salt concentration, $\frac{d\ln\gamma_{\pm}}{d\ln(m)}$, is small in this regime. Molecular dynamics simulations show that the most probable motif is one where each lithium ion is solvated by 6 ether oxygens in PEO.[69,70] At $r = 1/6 = 0.17$, all the available oxygens are coordinated with lithium ions. When the salt concentration exceeds this value, the average coordination environment of the lithium ions must necessarily be different from the most favorable configuration, including anion coordination. One expects this to result in a rapid change in the chemical potential of the salt. We attribute the rapid increase of $T_f$ in the $r > 0.17$ regime to this effect. In the limit of $r$ tending to 0, the electrolytes should be thermodynamically ideal and $T_f$

should approach unity. The Debye-Huckel theory indicates that $T_f$ should be less than 1 in sufficiently dilute electrolytes.[71] While our data are consistent with these expectations, the Debye-Huckel regime is outside the scope of our analysis.

The uncertainty in the fits in Figure 3 are represented by an approximate 95% confidence interval and shown as gray shading surrounding the fitted curves. They represent the uncertainty of the indirectly derived parameters $T_f$ and $t_{+}^{0}$ using Equation 1 and 2 based on the entire set of 64 samples. The uncertainty was obtained utilizing a Monte Carlo method.[72,73] We ran $10^5$ trials sampling values for $\kappa$, $D$, $\rho_+$, and $\frac{dU}{d\ln(m)}$ centered around their mean with standard deviations of

**Figure 3.** PEO/LiTFSI electrolyte properties at 90 °C of (a) cation transference number, $t_{+}^{0}$, as calculated by Equation 2 and (b) thermodynamic factor, $T_f$, as calculated by Equation 1. Data points are the properties determined at each individual molecular weight (circles/5 kg mol$^{-1}$; squares/10 kg mol$^{-1}$; diamonds/275 kg mol$^{-1}$) and the error bars correspond to one standard deviation. The black line is calculated from Equations 1-2 using the fitted Equations 4-7 and is shown for $r \geq 0.035$. 95% confidence intervals are given by the gray shading.

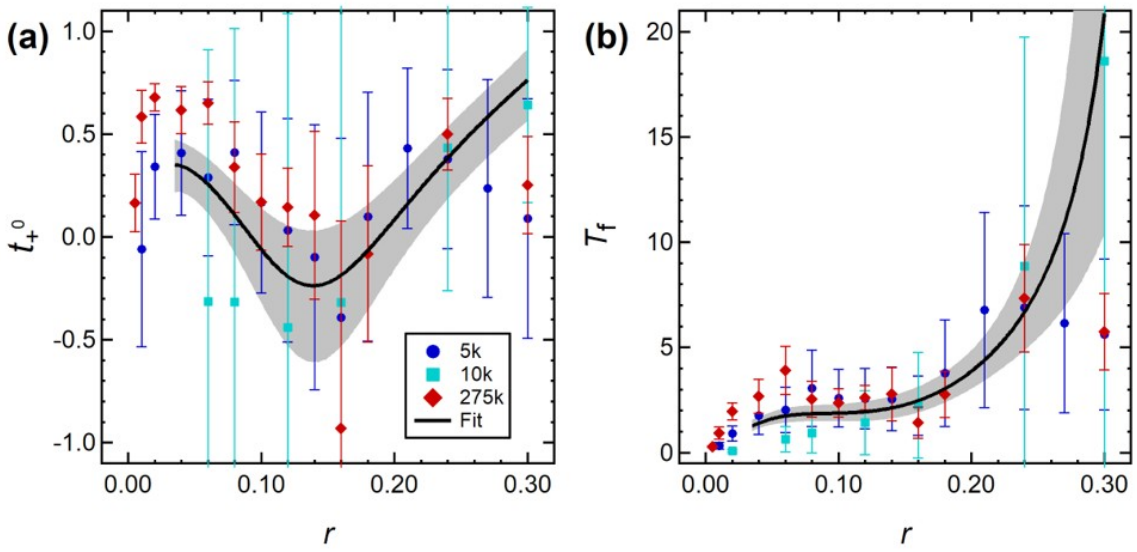


the fits of Equations 4-7 and calculated the resulting values for $T_f$ and $t_{+¿^0¿}$ using Equation 1 and 2 for each trial. The lower bound and upper bound of the 95% confidence interval is then given by the 2.5 and 97.5 percentile values in these trials. Details of our approach are given in the SI.

The curves in both Figures 3a and 3b only extend to $r$ = 0.035 in the dilute limit. At concentrations below this value, the curves are extremely sensitive to small changes in the fit parameters. In the dilute limit, $\rho_+$ approaches 0.18 and $\kappa$ is proportional to $c$, implying that the magnitude of $t_{+¿^0¿}$ depends crucially on the magnitude of $\frac{dU}{d\ln(m)}$ that appears in the denominator. However, $\frac{dU}{d\ln(m)}$ approaches a very small value in the dilute limit (see Figure 2d) and small changes in this value lead to very large changes in $t_{+¿^0¿}$. Similar problems arise when one examines Equation 1 for $T_f$ in the dilute limit. A parsimonious extrapolation of the curve representing the dependence of $t_{+¿^0¿}$ on $r$ suggests that the transference number in the limit of $r$ = 0 is 0.35. The fitted expression for $t_{+¿^0¿}$ does not give this result as it is affected by the scattered data at $r$ < 0.035. Despite these limitations, the complete electrochemical characterization of

three different sets of polymer electrolytes enable accurate quantification of ion transport over a large range of salt concentrations $0.035 \leq r \leq 0.30$. This is also the concentration range of practical relevance.

## 4. Conclusion

We have demonstrated that mixtures of lithium salt and entangled polymer chains are robust model systems for studying the fundamentals of ion transport. We present measurements of $\kappa$, $D$, $\rho_+$, and $\frac{dU}{d\ln(m)}$ of PEO/LiTFSI using 64 independent electrolyte samples with PEO molecular weights ranging from 5 to 275 kg mol$^{-1}$ and salt concentrations $0.005 \leq r \leq 0.3$. Current methods for determining these transport and thermodynamic parameters involve four separate experiments. The coupled nature of the equations used to determine the parameters results in large experimental uncertainty. A salient feature of this work is the rigorous quantification of experimental uncertainty. We minimize this uncertainty by taking advantage of the fact that transport and thermodynamics properties of polymer electrolytes above the entanglement threshold are independent of molecular weight. The dependence of transport parameters $\kappa$, $D$, $t_{+}^{0}$, and the thermodynamic factor, $T_f$, on salt concentration are presented with a confidence interval of 95%. $\kappa$, $D$, and $T_f$ are positive as required by the second law of thermodynamics. There are, however, no constraints on the sign of $t_{+}^{0}$. We find that $t_{+}^{0}$ is negative in the salt concentration window of $0.093 \leq r \leq 0.189$.

## Conflicts of Interest

The authors declare no competing financial interests.

## Acknowledgements

This work was intellectually led by the Joint Center for Energy Storage Research (JCESR), an Energy Innovation Hub funded by the U.S. Department of Energy, Office of Science, Office of Basic Energy Science, under Contract No. DE-AC02-06CH11357. K.W.G. acknowledges funding from a National Defense and Science Engineering Graduate Fellowship. The authors thank Michael D. Galluzzo, Zach J. Hoffman, Calvin Luo, Deep B. Shah, and Lorenzo N. Venneri for helpful discussions related to this work.

## References

(1) Onsager, L. Theories and Problems of Liquid Diffusion. *Ann. N. Y. Acad. Sci.* **1945**, *46* (5), 241–265. https://doi.org/10.1111/j.1749-6632.1945.tb36170.x.

(2) Newman, J.; Balsara, N. P. *Electrochemical Systems*, 4th ed.; John Wiley & Sons, Inc.: Hoboken, New Jersey, 2020.

(3) Ma, Y.; Doyle, M.; Fuller, T. F.; Doeff, M. M.; De Jonghe, L. C.; Newman, J. The Measurement of a Complete Set of Transport Properties for a Concentrated Solid Polymer Electrolyte Solution. *J. Electrochem. Soc.* **1995**, *142* (6), 1859–1868. https://doi.org/10.1149/1.2044206.

(4) Yokota, I. On the Theory of Mixed Conduction with Special Reference to the Conduction in Silver Sulfide Group Semiconductors. *J. Phys. Soc. Japan* **1961**, *16* (11), 2213–2223. https://doi.org/https://doi.org/10.1143/JPSJ.16.2213.

(5) Prigogine, I. *Introduction to Thermodynamics of Irreversible Processes*, 3rd ed.;

Interscience Publishers, Inc.: New York, 1967.

(6) de Groot, S. R.; Mazur, P. *Non-Equilibrium Thermodynamics*; Interscience Publishers, Inc.: New York, 1969.

(7) Maier, J.; Schwitzgebel, G. Theoretical Treatment of the Diffusion Coupled with Reaction, Applied to the Example of a Binary Solid Compound MX. *Phys. Status Solidi* **1982**, *113* (2), 535–547. https://doi.org/10.1002/pssb.2221130218.

(8) Kraaijeveld, G.; Wesselingh, J. A. Negative Maxwell-Stefan Diffusion Coefficients. *Ind. Eng. Chem. Res.* **1993**, *32* (4), 738–742. https://doi.org/10.1021/ie00016a022.

(9) Barthel, J. M. G.; Krienke, H.; Kunz, W. *Physical Chemistry of Electrolyte Solutions*; Springer: New York, 1998.

(10) Bockris, J. O.; Reddy, A. K. N. *Modern Electrochemistry*, 2nd ed.; Kluwer Academic Publishers: New York, 2002.

(11) Maier, J. Salt Concentration Polarization of Liquid Electrolytes and Determination of Transport Properties of Cations, Anions, Ion Pairs and Ion Triples. *Electrochim. Acta* **2014**, *129*, 21–27. https://doi.org/10.1016/j.electacta.2014.01.078.

(12) Fong, K. D.; Bergstrom, H. K.; McCloskey, B. D.; Mandadapu, K. K. Transport Phenomena in Electrolyte Solutions: Nonequilibrium Thermodynamics and Statistical Mechanics. *AIChE J.* **2020**, *66* (12), 1–50. https://doi.org/10.1002/aic.17091.

(13) Pfeifer, S.; Ackermann, F.; Sälzer, F.; Schönhoff, M.; Roling, B. Quantification of Cation-Cation, Anion-Anion and Cation-Anion Correlations in Li Salt/Glyme Mixtures by Combining Very-Low-Frequency Impedance Spectroscopy with Diffusion and Electrophoretic NMR. *Phys. Chem. Chem. Phys.* **2021**, *23* (1), 628–640.

https://doi.org/10.1039/d0cp06147f.

(14) Fong, R.; von Sacken, U.; Dahn, J. R. Studies of Lithium Intercalation into Carbons Using Nonaqueous Electrochemical Cells. *J. Electrochem. Soc.* **1990**, *137* (7), 2009–2013. https://doi.org/10.1149/1.2086855.

(15) Tarascon, J. M.; Guyomard, D. New Electrolyte Compositions Stable over the 0 to 5 V Voltage Range and Compatible with the Li1+xMn2O4/Carbon Li-Ion Cells. *Solid State Ionics* **1994**, *69* (3–4), 293–305. https://doi.org/10.1016/0167-2738(94)90418-9.

(16) Xu, K. Nonaqueous Liquid Electrolytes for Lithium-Based Rechargeable Batteries. *Chem. Rev.* **2004**, *104*, 4303–4417. https://doi.org/10.1021/cr030203g.

(17) Xie, J.; Lu, Y. C. A Retrospective on Lithium-Ion Batteries. *Nat. Commun.* **2020**, *11* (1), 9–12. https://doi.org/10.1038/s41467-020-16259-9.

(18) Doyle, M.; Fuller, T. F.; Newman, J. The Importance of the Lithium Ion Transference Number in Lithium/Polymer Cells. *Electrochim. Acta* **1994**, *39* (13), 2073–2081. https://doi.org/10.1016/0013-4686(94)85091-7.

(19) Shah, D. B.; Kim, H. K.; Nguyen, H. Q.; Srinivasan, V.; Balsara, N. P. Comparing Measurements of Limiting Current of Electrolytes with Theoretical Predictions up to the Solubility Limit. *J. Phys. Chem. C* **2019**, *123* (39), 23872–23881. https://doi.org/10.1021/acs.jpcc.9b07121.

(20) Pesko, D. M.; Feng, Z.; Sawhney, S.; Newman, J.; Srinivasan, V.; Balsara, N. P. Comparing Cycling Characteristics of Symmetric Lithium-Polymer-Lithium Cells with Theoretical Predictions. *J. Electrochem. Soc.* **2018**, *165* (13), A3186–A3194. https://doi.org/10.1149/2.0921813jes.

(21) Gribble, D. A.; Frenck, L.; Shah, D. B.; Maslyn, J. A.; Loo, W. S.; Mongcopa, K. I. S.; Pesko, D. M.; Balsara, N. P. Comparing Experimental Measurements of Limiting Current in Polymer Electrolytes with Theoretical Predictions. *J. Electrochem. Soc.* **2019**, *166* (14), A3228–A3234. https://doi.org/10.1149/2.0391914jes.

(22) Kondo, K.; Sano, M.; Hiwara, A.; Omi, T.; Fujita, M.; Kuwae, A.; Iida, M.; Mogi, K.; Yokoyama, H. Conductivity and Solvation of Li + Ions of LiPF6 in Propylene Carbonate Solutions. *J. Phys. Chem. B* **2000**, *104*, 5040–5044. https://doi.org/10.1021/jp000142f.

(23) Stewart, S.; Newman, J. Measuring the Salt Activity Coefficient in Lithium-Battery Electrolytes. *J. Electrochem. Soc.* **2008**, *155* (6), A458. https://doi.org/10.1149/1.2904526.

(24) Nishida, T.; Nishikawa, K.; Fukunaka, Y. Diffusivity Measurement of LiPF6, LiTFSI, LiBF4 in PC. *ECS Trans.* **2008**, *6* (18), 1–14. https://doi.org/10.1149/1.2831921.

(25) Hwang, S.; Kim, D.; Shin, J. H.; Jang, J. E.; Ahn, K. H.; Lee, C.; Lee, H. Ionic Conduction and Solution Structure in LiPF6 and LiBF4 Propylene Carbonate Electrolytes. *J. Phys. Chem. C* **2018**, *122*, 19438–19446. https://doi.org/10.1021/acs.jpcc.8b06035.

(26) Hou, T.; Monroe, C. W. Composition-Dependent Thermodynamic and Mass-Transport Characterization of Lithium Hexafluorophosphate in Propylene Carbonate. *Electrochim. Acta* **2020**, *332*, 135085. https://doi.org/10.1016/j.electacta.2019.135085.

(27) Shah, D. B. Ion Transport Properties in Novel and Traditional Liquid Electrolytes for Lithium-Based Batteries, University of California, Berkeley, 2020.

(28) Liu, Q.; Du, C.; Shen, B.; Zuo, P.; Cheng, X.; Ma, Y.; Yin, G.; Gao, Y. Understanding Undesirable Anode Lithium Plating Issues in Lithium-Ion Batteries. *RSC Adv.* **2016**, *6* (91), 88683–88700. https://doi.org/10.1039/c6ra19482f.

(29) Cheng, X. B.; Zhang, R.; Zhao, C. Z.; Wei, F.; Zhang, J. G.; Zhang, Q. A Review of Solid Electrolyte Interphases on Lithium Metal Anode. *Adv. Sci.* **2015**, *3* (3), 1–20. https://doi.org/10.1002/advs.201500213.

(30) Zhai, P.; Liu, L.; Gu, X.; Wang, T.; Gong, Y. Interface Engineering for Lithium Metal Anodes in Liquid Electrolyte. *Adv. Energy Mater.* **2020**, *10* (34), 1–32. https://doi.org/10.1002/aenm.202001257.

(31) Galluzzo, M. D.; Maslyn, J. A.; Shah, D. B.; Balsara, N. P. Ohm's Law for Ion Conduction in Lithium and beyond-Lithium Battery Electrolytes. *J. Chem. Phys.* **2019**, *151* (2). https://doi.org/10.1063/1.5109684.

(32) Wang, A. A.; Hou, T.; Karanjavala, M.; Monroe, C. W. Shifting-Reference Concentration Cells to Refine Composition-Dependent Transport Characterization of Binary Lithium-Ion Electrolytes. *Electrochim. Acta* **2020**, *358*, 136688. https://doi.org/10.1016/j.electacta.2020.136688.

(33) Zhao, J.; Wang, L.; He, X.; Wan, C.; Jiang, C. Determination of Lithium-Ion Transference Numbers in LiPF6–PC Solutions Based on Electrochemical Polarization and NMR Measurements. *J. Electrochem. Soc.* **2008**, *155* (4), A292. https://doi.org/10.1149/1.2837832.

(34) de Gennes, P. G. *Scaling Concepts in Polymer Chemistry*; Cornell University Press: Ithaca, NY, 1979.

(35) Wool, R. P. Polymer Entanglements. *Macromolecules* **1993**, *26* (7), 1564–1569. https://doi.org/10.1021/ma00059a012.

(36) Shi, J.; Vincent, C. A. The Effect of Molecular Weight on Cation Mobility in Polymer

Electrolytes. *Solid State Ionics* **1993**, *60* (1–3), 11–17. https://doi.org/10.1016/0167-2738(93)90268-8.

(37) Teran, A. A.; Tang, M. H.; Mullin, S. A.; Balsara, N. P. Effect of Molecular Weight on Conductivity of Polymer Electrolytes. *Solid State Ionics* **2011**, *203* (1), 18–21. https://doi.org/10.1016/j.ssi.2011.09.021.

(38) Chattoraj, J.; Knappe, M.; Heuer, A. Dependence of Ion Dynamics on the Polymer Chain Length in Poly(Ethylene Oxide)-Based Polymer Electrolytes. *J. Phys. Chem. B* **2015**, *119* (22), 6786–6791. https://doi.org/10.1021/jp512734g.

(39) Newman, J.; Chapman, T. W. Restricted Diffusion in Binary Solutions. *AIChE J.* **1973**, *19* (2), 343–348. https://doi.org/10.1002/aic.690190220.

(40) Bruce, P. G.; Hardgrave, M. T.; Vincent, C. A. Steady State Current Flow in Solid Binary Electrolyte Cells. *J. Electroanal. Chem. Interfacial Electrochem.* **2002**, *271* (1–2), 27–34. https://doi.org/10.1016/0022-0728(89)80061-0.

(41) Evans, J.; Vincent, C. A.; Bruce, P. G. Electrochemical Measurement of Transference Numbers in Polymer Electrolytes. *Polymer (Guildf).* **1987**, *28* (13), 2324–2328. https://doi.org/10.1016/0032-3861(87)90394-6.

(42) Pesko, D. M.; Timachova, K.; Bhattacharya, R.; Smith, M. C.; Villaluenga, I.; Newman, J.; Balsara, N. P. Negative Transference Numbers in Poly(Ethylene Oxide)-Based Electrolytes. *J. Electrochem. Soc.* **2017**, *164* (11), E3569–E3575. https://doi.org/10.1149/2.0581711jes.

(43) Chintapalli, M.; Le, T. N. P.; Venkatesan, N. R.; Mackay, N. G.; Rojas, A. A.; Thelen, J. L.; Chen, X. C.; Devaux, D.; Balsara, N. P. Structure and Ionic Conductivity of

Polystyrene-Block-Poly(Ethylene Oxide) Electrolytes in the High Salt Concentration Limit. *Macromolecules* **2016**, *49* (5), 1770–1780. https://doi.org/10.1021/acs.macromol.5b02620.

(44) Pesko, D. M.; Sawhney, S.; Newman, J.; Balsara, N. P. Comparing Two Electrochemical Approaches for Measuring Transference Numbers in Concentrated Electrolytes. *J. Electrochem. Soc.* **2018**, *165* (13), A3014–A3021. https://doi.org/10.1149/2.0231813jes.

(45) Hoffman, Z. J.; Shah, D. B.; Balsara, N. P. Temperature and Concentration Dependence of the Ionic Transport Properties of Poly(Ethylene Oxide) Electrolytes. *Solid State Ionics.* In preparation.

(46) Zheng, Q.; Pesko, D. M.; Savoie, B. M.; Timachova, K.; Hasan, A. L.; Smith, M. C.; Miller, T. F.; Coates, G. W.; Balsara, N. P. Optimizing Ion Transport in Polyether-Based Electrolytes for Lithium Batteries. *Macromolecules* **2018**, *51* (8), 2847–2858. https://doi.org/10.1021/acs.macromol.7b02706.

(47) Ku, H. H. Notes on the Use of Propagation of Error Formulas. *J. Res. Natl. Bur. Stand. - C. Eng. Instrum.* **1966**, *70* (4), 75–79. https://doi.org/10.6028/jres.070c.025.

(48) Mongcopa, K. I. S.; Tyagi, M.; Mailoa, J. P.; Samsonidze, G.; Kozinsky, B.; Mullin, S. A.; Gribble, D. A.; Watanabe, H.; Balsara, N. P. Relationship between Segmental Dynamics Measured by Quasi- Elastic Neutron Scattering and Conductivity in Polymer Electrolytes. *ACS Macro Lett.* **2018**, *7*, 504–508. https://doi.org/10.1021/acsmacrolett.8b00159.

(49) Lascaud, S.; Perrier, M.; Vallée, A.; Besner, S.; Prud′homme, J.; Armand, M. Phase Diagrams and Conductivity Behavior of Poly(Ethylene Oxide)-Molten Salt Rubbery

Electrolytes. *Macromolecules* **1994**, *27* (25), 7469–7477. https://doi.org/10.1021/ma00103a034.

(50) Fullerton-Shirey, S. K.; Maranas, J. K. Effect of LiClO4 on the Structure and Mobility of PEO-Based Solid Polymer Electrolytes. *Macromolecules* **2009**, *42* (6), 2142–2156. https://doi.org/10.1021/ma802502u.

(51) Robitaille, C. D.; Fauteux, D. Phase Diagrams and Conductivity Characterization of Some PEO-LiX Electrolytes. *J. Electrochem. Soc.* **1986**, *133* (2), 315–325. https://doi.org/10.1149/1.2108569.

(52) Pożyczka, K.; Marzantowicz, M.; Dygas, J. R.; Krok, F. IONIC CONDUCTIVITY AND LITHIUM TRANSFERENCE NUMBER OF POLY(ETHYLENE OXIDE):LiTFSI SYSTEM. *Electrochim. Acta* **2017**, *227*, 127–135. https://doi.org/10.1016/j.electacta.2016.12.172.

(53) Devaux, D.; Bouchet, R.; Glé, D.; Denoyel, R. Mechanism of Ion Transport in PEO/LiTFSI Complexes: Effect of Temperature, Molecular Weight and End Groups. *Solid State Ionics* **2012**, *227*, 119–127. https://doi.org/10.1016/j.ssi.2012.09.020.

(54) Schantz, S.; Torell, L. M.; Stevens, J. R. Ion Pairing Effects in Poly(Propylene Glycol)-Salt Complexes as a Function of Molecular Weight and Temperature: A Raman Scattering Study Using NaCF3SO3 and LiClO4. *J. Chem. Phys.* **1991**, *94* (10), 6862–6867. https://doi.org/10.1063/1.460265.

(55) Ratner, M. A.; Johansson, P.; Shriver, D. F. Polymer Electrolytes: Ionic Transport Mechanisms and Relaxation Coupling. *MRS Bull.* **2000**, *25*, 31–37. https://doi.org/10.1557/mrs2000.16.

(56) Gao, K. W.; Jiang, X.; Hoffman, Z. J.; Sethi, G. K.; Chakraborty, S.; Villaluenga, I.; Balsara, N. P. Optimizing the Monomer Structure of Polyhedral Oligomeric Silsesquioxane for Ion Transport in Hybrid Organic–Inorganic Block Copolymers. *J. Polym. Sci.* **2020**, *58* (2), 363–371. https://doi.org/10.1002/pol.20190073.

(57) Gouverneur, M.; Schmidt, F.; Schönhoff, M. Negative Effective Li Transference Numbers in Li Salt/Ionic Liquid Mixtures: Does Li Drift in the "Wrong" Direction? *Phys. Chem. Chem. Phys.* **2018**, *20*, 7470–7478. https://doi.org/10.1039/c7cp08580j.

(58) Molinari, N.; Mailoa, J. P.; Kozinsky, B. Effect of Salt Concentration on Ion Clustering and Transport in Polymer Solid Electrolytes: A Molecular Dynamics Study of PEO-LiTFSI. *Chem. Mater.* **2018**, *30* (18), 6298–6306. https://doi.org/10.1021/acs.chemmater.8b01955.

(59) Galluzzo, M. D.; Loo, W. S.; Wang, A. A.; Walton, A.; Maslyn, J. A.; Balsara, N. P. Measurement of Three Transport Coefficients and the Thermodynamic Factor in Block Copolymer Electrolytes with Different Morphologies. *J. Phys. Chem. B* **2020**, *124* (5), 921–935. https://doi.org/10.1021/acs.jpcb.9b11066.

(60) France-Lanord, A.; Wang, Y.; Xie, T.; Johnson, J. A.; Shao-Horn, Y.; Grossman, J. C. Effect of Chemical Variations in the Structure of Poly(Ethylene Oxide)-Based Polymers on Lithium Transport in Concentrated Electrolytes. *Chem. Mater.* **2020**, *32* (1), 121–126. https://doi.org/10.1021/acs.chemmater.9b02645.

(61) Kim, H.-K.; Balsara, N. P.; Srinivasan, V. Continuum Description of the Role of Negative Transference Numbers on Ion Motion in Polymer Electrolytes. *J. Electrochem. Soc.* **2020**, *167* (11), 110559. https://doi.org/10.1149/1945-7111/aba790.

(62) MacCallum, J. R.; Tomlin, A. S.; Vincent, C. A. An Investigation of the Conducting Species in Polymer Electrolytes. *Eur. Polym. J.* **1986**, *22* (10), 787–791. https://doi.org/10.1016/0014-3057(86)90017-0.

(63) Gray, F. Conductance and Conducting Species in Amorphous Polyether-Lithium Perchlorate Systems at Very Low Salt Concentration. *Solid State Ionics* **1990**, *40–41*, 637–640. https://doi.org/10.1016/0167-2738(90)90086-7.

(64) Bruce, P. G. Ion Association in Polymer Electrolytes: Transport and Materials Optimization. *Synth. Met.* **1991**, *45* (3), 267–278. https://doi.org/10.1016/0379-6779(91)91783-7.

(65) Irish, D. E.; McCarroll, B.; Young, T. F. Raman Study of Zinc Chloride Solutions. *J. Chem. Phys.* **1963**, *39* (12), 3436–3444. https://doi.org/10.1063/1.1734212.

(66) Spiro, T. G. A Raman Study of Thallium(III) Chloride Complexes in Aqueous Solution. *Inorg. Chem.* **1965**, *4* (5), 731–738. https://doi.org/10.1021/ic50027a029.

(67) Oertel, R. P.; Plane, R. A. Raman Study of Chloride and Bromide Complexes of Bismuth(III). *Inorg. Chem.* **1967**, *6* (11), 1960–1967. https://doi.org/10.1021/ic50057a004.

(68) Molinari, N.; Mailoa, J. P.; Kozinsky, B. General Trend of a Negative Li Effective Charge in Ionic Liquid Electrolytes. *J. Phys. Chem. Lett.* **2019**, *10* (10), 2313–2319. https://doi.org/10.1021/acs.jpclett.9b00798.

(69) Borodin, O.; Smith, G. D. Mechanism of Ion Transport in Amorphous Poly(Ethylene Oxide)/LiTFSI from Molecular Dynamics Simulations. *Macromolecules* **2006**, *39*, 1620–1629. https://doi.org/10.1021/ma052277v.

(70) Webb, M. A.; Savoie, B. M.; Wang, Z. G.; Miller, T. F. Chemically Specific Dynamic Bond Percolation Model for Ion Transport in Polymer Electrolytes. *Macromolecules* **2015**, *48* (19), 7346–7358. https://doi.org/10.1021/acs.macromol.5b01437.

(71) Debye, P. J. W.; Huckel, E. *The Collected Papers of Peter J. W. Debye*; 1954. https://doi.org/10.1161/01.res.2.2.185.

(72) Efron, B. Nonparametric Estimates of Standard Error: The Jacknife, the Bootstrap and Other Methods. *Biometrika* **1981**, *68* (3), 589–599. https://doi.org/10.1016/0045-6535(85)90163-8.

(73) Press, W. H.; Teukolsky, S. A.; Vetterling, W. T.; Flannery, B. P. *Numerical Recipes: The Art of Scientific Computing*, 3rd ed.; Cambridge University Press, 2007.